research articles Journal of proteome research

# Systems Responses of Rats to Aflatoxin B1 Exposure Revealed with Metabonomic Changes in Multiple Biological Matrices

**Limin Zhang,[†] Yangfang Ye,[†,‡] Yanpeng An,[†,§] Yuan Tian,[†,§] Yulan Wang,[*,†] and Huiru Tang[*,†]**

*State Key Laboratory of Magnetic Resonance and Atomic and Molecular Physics, Wuhan Centre for Magnetic Resonance, Wuhan Institute of Physics and Mathematics, Chinese Academy of Sciences, Wuhan 430071, P. R. China, Graduate University of the Chinese Academy of Sciences, Beijing 100049, P. R. China, and Key Laboratory of Applied Marine Biotechnology of Ministry of Education, Ningbo University, Ningbo 315211, P. R. China*

**Received July 30, 2010**

Exposure to aflatoxins causes liver fibrosis and hepatocellular carcinoma posing a significant health risk for human populations and livestock. To understand the mammalian systems responses to aflatoxin-B1 (AFB1) exposure, we analyzed the AFB1-induced metabonomic changes in multiple biological matrices (plasma, urine, and liver) of rats using $^1$H NMR spectroscopy together with clinical biochemistry and histopathologic assessments. We found that AFB1 exposure caused significant elevation of glucose, amino acids, and choline metabolites (choline, phosphocholine, and glycerophosphocholine) in plasma but reduction of plasma lipids. AFB1 also induced elevation of liver lipids, amino acids (tyrosine, histidine, phenylalanine, leucine, isoleucine, and valine), choline, and nucleic acid metabolites (inosine, adenosine, and uridine) together with reduction of hepatic glycogen and glucose. AFB1 further caused decreases in urinary TCA cycle intermediates (2-oxoglutarate and citrate) and elevation of gut microbiota cometabolites (phenylacetylglycine and hippurate). These indicated that AFB1 exposure caused hepatic steatosis accompanied with widespread metabolic changes including lipid and cell membrane metabolisms, protein biosynthesis, glycolysis, TCA cycle, and gut microbiota functions. This implied that AFB1 exposure probably caused oxidative-stress-mediated impairments of mitochondria functions. These findings provide an overview of biochemical consequences of AFB1 exposure and comprehensive insights into the metabolic aspects of AFB1-induced hepatotoxicity in rats.

**Keywords:** hepatotoxicology • metabonomics • aflatoxin B1 • nuclear magnetic resonance (NMR)

## Introduction

Aflatoxins are produced by fungi, such as *Aspergillus flavus* and *Aspergillus parasiticus*,[1] and commonly found in food and feedstuff[2] containing cereal grains, oilseeds, and peanuts in humid environments. The exposure to aflatoxins can lead to liver injuries, liver fibrosis, and hepatocellular carcinoma (HCC) and hence poses a significant health risk for human populations and livestock.[3,4] There are many natural aflatoxins such as aflatoxin B1, B2, G1, and G2, among which aflatoxin B1 (AFB1) is the most frequently occurring and highly toxic one.[5,6]

Traditional biochemical studies have shown that the hepatotoxicity of AFB1 is related to its interactions with biomolecules such as nucleic acid and proteins.[7−9] AFB1 is initially oxidized by the microsomal mono-oxygenases in the liver cytochrome P450 system,[10,11] yielding highly reactive AFB1-*exo*-8,9-epoxide as the ultimate carcinogen. AFB1-*exo*-8,9-epoxide is a short-lived electrophile and can readily form an 8,9-dihydro-8-($N^7$-guanyl)-9-hydroxy-AFB1 (AFB1-$N^7$-Gua) adduct by binding to the guanine residues of DNA.[7] AFB1-*exo*-8,9-epoxide can also undergo rapid nonenzymatic hydrolysis to form AFB1-dihydrodiol,[12] which in turn undergoes slow base-catalyzed ring-opening to form a dialdehyde phenolate ion. Such an ion can interact with protein amine groups to form AFB1−protein adducts, such as aflatoxin−albumin.[13] The formation of these DNA and protein adducts causes serious DNA, RNA, and proteins dysfunctions.[14−16]

Consequently, AFB1 exposure causes alterations in metabolic processes, such as glycogenolysis/glycolysis[17] and phospholipidation,[18] and changes in amino acid transportation.[14] AFB1 exposure can also indirectly result in damages to the structural integrity of cell membranes and ultimately lead to cell death.[19] Therefore, AFB1 exposure may cause changes in metabolisms related to the cell membrane although no such reports have been published so far. With the traditional biochemical method focusing on a single metabolic pathway at a time,[17] however, it remains to be systematically investigated whether AFB1 exposure causes other metabolic alterations especially me-

* To whom correspondence should be addressed. H.T.: e-mail, Huiru.tang@wipm.ac.cn; tel, +86-27-87198430; fax, +86-27-87199291. Y.W.: e-mail, Yulan.wang@wipm.ac.cn; tel, +86-27-87197143; fax, +86-27-87199291.

† State Key Laboratory of Magnetic Resonance and Atomic and Molecular Physics.

‡ Ningbo University.

§ Graduate School of the Chinese Academy of Sciences.


10.1021/pr100792q 
Published on Web 11/17/2010

tabolism of lipids, choline, and nucleic acids. A holistic systems approach is useful to answer these questions and to further our understanding of metabolic effects of AFB1 *in vivo*. The newly established metabonomic technology should be a suitable tool as indicated in investigations of systems metabolic responses to many toxins and related mechanisms.[20−23]

Technically, metabonomics involves an analysis of metabolic profiles of biofluids or tissue extracts using $^1$H NMR spectroscopy or mass spectrometry in conjunction with multivariate data analysis.[24] NMR has been extensively used in metabonomic analysis for biofluids and tissues since it is nonselective to detectable metabolites, reproducible, rich in structural information, and quantitative. NMR can also be used to detect metabolic components from intact tissue, such as a biopsy of liver or kidney, providing the molecular information associated with pathological consequence. This is achieved by spinning tissue samples at the "magic angle (54.7°)" (MAS) with respect to a magnetic field so as to produce high resolution NMR spectra from soft tissues by averaging out a range of NMR line broadening factors, such as dipolar−dipolar interactions, chemical shift anisotropy, and magnetic field inhomogeneity. For example, the metabolic features of human hepatocellular carcinoma (HCC) were recently characterized employing $^1$H high resolution MAS NMR spectroscopy in conjunction with pattern recognition (PR) techniques.[25] Similar approaches have also been applied to study the organ-specific biochemical responses to a number of toxins such as hydrazine,[26] acetaminophen,[27] and perfluorododecanoic acid (PFDoA).[28]

In the present study, we analyzed the AFB1-induced metabonomic changes in rat urine, plasma, liver tissues and their extracts using NMR-based metabonomic approaches coupled with clinical chemistry information and histopathological assessments of liver tissues. The objectives are to investigate the multiple-matrix metabolic responses of rats to AFB1 exposure and to further our understanding of the AFB1 toxicity at the systems level.

## Materials and Methods

**Chemicals.** Sodium chloride, $K_2HPO_4 \cdot 3H_2O$, and $NaH_2PO_4 \cdot 2H_2O$ (all in analytical grade) were obtained from Guoyao Chemical Co. Ltd. (Shanghai, China). Sodium 3-trimethylsilyl [2,2,3,3-$d_4$] propionate (TSP-$d_4$) and $D_2O$ (99.9% in D) were purchased from Cambridge Isotope Laboratories (Miami, FL).

**Animal Experiments and Sample Collection.** Animal experimental procedures were performed according to the National Guidelines for Experimental Animal Welfare (MOST of People's Republic of China, 2006) and were approved by the Local Animal Welfare Committee with permission No. SYXK (E) 2009-0051. A total of 27 male Sprague−Dawley (SD) rats (170−220 g, 7 weeks old) were purchased from Tongji Medical College, Huazhong University of Science and Technology, and housed in groups of five at a certified local animal experimental laboratory with a 12 h light/dark cycle at constant temperature of 23 ± 1 °C. Animals were allowed to have free access to food and water. After acclimatization for 4 weeks, rats were randomly divided into two groups and subjected to treatments for 12 days; controls ($n$ = 13) were fed with normal chow and the treatment group ($n$ = 14) with chow containing 1.6 ppm AFB1 (1.6 mg/kg food), which was purchased from Ruixin Agricultural Science and Trade Co., Beijing, China. Daily food consumption was monitored for rats and the average AFB1 intake was about 0.32 mg/(kg body weight/day).

The urine samples were collected every other day (i.e., day 1, 3, 5, 7, 9 and 11) over the AFB1 treatment period with the addition of 20 μL sodium azide solution (0.5% w/v). At the end of experimental period (day 12), all animals were sacrificed by cervical dislocation under isoflurane anesthesia following 12 h fasting. Blood samples were collected from the orbital plexus into Eppendorf tubes containing sodium heparin to obtain plasma samples with standard centrifugation procedures, and were stored at −80 °C for later analysis. Serum samples were also obtained for clinical biochemistry examination using standard procedures. Liver was removed from each animal and weighed; duplicate samples from the left lateral liver lobe were excised, one of which was immediately snap-frozen in liquid nitrogen and stored at −80 °C for later NMR analysis while the other one was fixed in 10% formalin solution for histopathological assessments.

**Histopathology and Clinical Biochemistry.** The formalin-fixed liver biopsies were embedded in paraffin wax, sectioned (3−4 μm), and stained with hematoxylin and eosin (H & E) followed with examination under a microscope by a qualified pathologist (as a paid service).

Clinical biochemistry analysis was done with a HITEC Integra 7080 automatic analyzer (Hitec Ltd., Hitachi, Japan) including alanine aminotransferase (ALT), aspartate aminotransferase (AST), albumin (ALB), bilirubin (D-BIL), urea nitrogen (BUN), glucose (Glc), triglycerides (TG), total cholesterol (CHOL), HDL-C, LDL-C, and creatinine (Cr). Obtained data were analyzed using SPSS 13.0 software with a Tukey post-test (one way-ANOVA) to test discrimination significances between the control and the treatment group.

**Sample Preparation for NMR Spectroscopy.** Plasma samples were prepared by mixing 200 μL plasma with 400 μL saline solution containing 10% $D_2O$; 550 μL samples was transferred into 5 mm NMR tubes after vortexing and centrifugation (11 180*g*, 10 min, 4 °C).

A total of 550 μL urine sample was mixed with 55 μL phosphate buffer ($K_2HPO_4/NaH_2PO_4$, 1.5 M, pD 7.4, 50% v/v $D_2O$)[29] containing 0.005% TSP-$d_4$ as chemical shift reference ($\delta$ 0.00 ppm). After centrifugation at 16 099*g* for 10 min, the supernatant was pipetted into 5 mm NMR tubes for NMR analysis.

Tissue samples (10−15 mg) were rinsed with sufficient saline in $D_2O$ and packed into 4 mm zirconia rotors for HR MAS NMR analysis.

Liver tissues (∼60 mg) were extracted twice with 1 mL 50% aqueous acetonitrile using a tissue-lyzer (Qiagen TissueLyser, Retsch GmBH, Germany). After centrifugation at 11 180*g* for 10 min at 4 °C, the combined supernatants were lyophilized after removing acetonitrile *in vacuo*. Each of the aqueous liver extracts was separately reconstituted into 600 μL phosphate buffer (0.1 M, $K_2HPO_4/NaH_2PO_4$ and pD 7.4) containing 10% $D_2O$, 0.005% TSP-$d_4$, and 0.2% $NaN_3$. Following centrifugation, 550 μL such solution of each extract was transferred into 5 mm NMR tubes.

**$^1$H NMR Spectroscopy.** $^1$H NMR spectra of urine, plasma, and aqueous liver extracts were recorded at 300 K on a Bruker Avance III 600 MHz spectrometer (operating at 600.13 MHz for $^1$H) equipped with a Bruker inverse cryogenic probe, whereas $^1$H HRMAS NMR spectra of intact liver tissue were acquired at 283 K on a Varian INOVA-600 spectrometer with a Varian Nanoprobe and spinning rate of 2.5 kHz (due to hardware restriction). For urine and aqueous liver extracts, a standard water-suppressed one-dimensional NMR spectrum

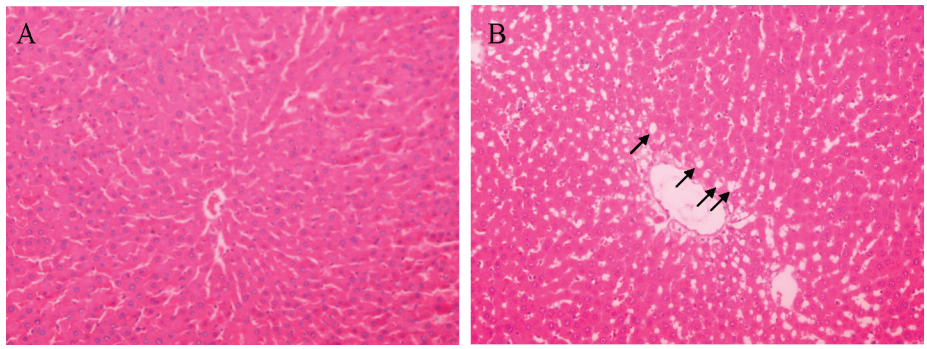


**Figure 1.** Hepatic histopathology. Light micrographs (×200) of (A) control, (B) AFB1 treated (0.32 mg/(kg/d)). Arrows indicate vacuolation in the periportal hepatocytes.

was recorded using the first increment of NOESY pulse sequence (recycle delay-90°-$t_1$-90°-$t_m$-90°-acquisition) with recycle delay of 2 s, $t_1$ of 3 $\mu$s and the mixing time, $t_m$, of 100 ms. For plasma and liver tissues, a water-presaturated Carr−Purcell−Meiboom−Gill (CPMG) pulse sequence (recycle delay-90°-($\tau$-180°-$\tau$)$_n$-acquisition) was employed to attenuate NMR signals from macromolecules. The spin−spin relaxation delays ($2n\tau$) of 96 and 100 ms were used for plasma and liver tissues, respectively. Typically, 90° pulse was set to about 10.0 $\mu$s and 64 transients were collected into 32K data points for each spectrum with a spectral width of 20 ppm. All free induction decays were multiplied by an exponential function with a 1 Hz line broadening factor prior to Fourier transformation. The spectra were referenced to TSP-$d_4$ at $\delta$0.00 when TSP-$d_4$ was present. Otherwise, the chemical shift of anomeric proton signal of α-glucose ($\delta$ 5.233) was used as chemical shift reference. To facilitate NMR signal assignments, a range of 2D NMR spectra were acquired and processed as described previously[28,30,31] for selected samples including $^1$H−$^1$H correlation spectroscopy (COSY), $^1$H−$^1$H total correlation spectroscopy (TOCSY), $^1$H−$^{13}$C heteronuclear single quantum correlation (HSQC), and $^1$H−$^{13}$C heteronuclear multiple bond correlation spectra (HMBC).

**NMR Data Processing and Multivariate Data Analysis.** All the $^1$H NMR spectra were corrected manually for phase and baseline distortions and spectral region $\delta$ 0.5−9.5 was integrated into regions with equal width of 0.004 ppm (2.4 Hz) using AMIX software package (V3.8, Bruker-Biospin, Germany). Regions distorted by imperfect water saturation were discarded with the regions containing urea signals. These regions are $\delta$ 4.12−5.21 for plasma, $\delta$ 4.50−5.30 and $\delta$ 5.50−6.00 for urine, $\delta$ 4.70−5.15 for intact liver tissue, and $\delta$ 4.20−5.15 for aqueous liver extracts. Each bucketed region was then normalized to the total sum of the spectral integrals to compensate for the overall concentration differences prior to statistical data analysis.

Multivariate data analysis was carried out with the SIMCA-P$^+$ software (version 11.0, Umetrics, Sweden). Principal Component Analysis (PCA) was initially carried out on mean-centered NMR data to generate an overview. Orthogonal Projection to Latent Structure with Discriminant Analysis (O-PLS-DA) was subsequently conducted using NMR data (scaled to unit variance) as **X**-matrix and class information as **Y**-matrix. The O-PLS-DA models were validated using a 6-fold cross-validation method[32] and further evaluated with a permutation test (200 permutations).[33] To facilitate interpretation of the results, the loadings that indicate altered metabolites after treatment were back-transformed and plotted with a color-coded correlation coefficient for each data point using an in-house developed Matlab script (V7.1, the Math-works, MA). The color-coded correlation coefficient indicates the significance of the metabolite contribution to the class separation, with a "hot" color (e.g., red) being more significant than a "cold" color (e.g., blue). In this study, a cutoff value of $|r| > 0.514$ ($r > 0.514$ and $r < -0.514$) was chosen for correlation coefficient as significant based on the discrimination significance ($p < 0.05$).

## Results

**Histopathology and Clinical Biochemistry.** Figure 1 shows that rats exposed to AFB1 have developed typical liver steatosis with lipid droplets and vacuolated hepatocytes (Figure 1B) as compared to the control rats. Clinical biochemistry results indicated that the AFB1-treated rats had significantly higher serum levels of ALT, AST, D-BIL, BUN, CHOL, and Glc but lower level of TG than controls. No significant changes were observed in the levels of ALB, Cr, HDL-C, and LDL-C (Supporting Information Table S1).

**Metabolite Assignments with $^1$H NMR Spectroscopy.** Figure 2 shows some typical $^1$H NMR spectra for blood plasma, intact liver tissue, and liver extracts obtained from a control rat ($P_A$, $L_A$, $E_A$) and an AFB1-treated rat ($P_B$, $L_B$, $E_B$). The metabolite resonances were assigned according to literature[28,34] and confirmed with a series of 2D NMR experiments with both $^1$H and $^{13}$C data shown in Supporting Information Table S2. Plasma spectra (Figure 2, $P_A$ and $P_B$) showed signals from mainly lipoproteins, glycoproteins, glucose, amino acids, carboxylic acids such as lactate and D-3-hydroxybutyrate (3-HB), and choline metabolites. $^1$H HRMAS NMR spectra of intact liver tissues (Figure 2, $L_A$ and $L_B$) contained peaks from glucose, glycogen, choline, phosphocholine (PC), glycerophosphocholine (GPC), 3-HB, lactate, TMAO, betaine, and lipid moieties. In the $^1$H NMR spectra of aqueous liver extracts (Figure 2, $E_A$ and $E_B$), additional peaks were clearly observed for nucleotide metabolites, such as inosine, adenosine, and uridine apart from those metabolites observed in Figure 2, $L_A$−$L_B$. Visual inspection of these spectra revealed that the AFB1 treated rat had lower hepatic glucose and glycogen levels but higher lipid levels than control rat (Figure 2, $L_A$ and $L_B$). Analysis of NMR profiles for the kidney tissues and extracts did not show significant metabonomic changes induced by AFB1 treatment (data not shown).

Figure 3 shows some representative $^1$H NMR spectra of urine samples obtained from an AFB1 dosed rat at various time points (predose, day 3, day 7 and day 11 postdose, respectively). Main peaks observed were from ketone bodies (3-HB, acetoacetate), hippurate and various organic acids including 2-oxoglutarate, citrate, succinate, fumarate, lactate, and creatine.

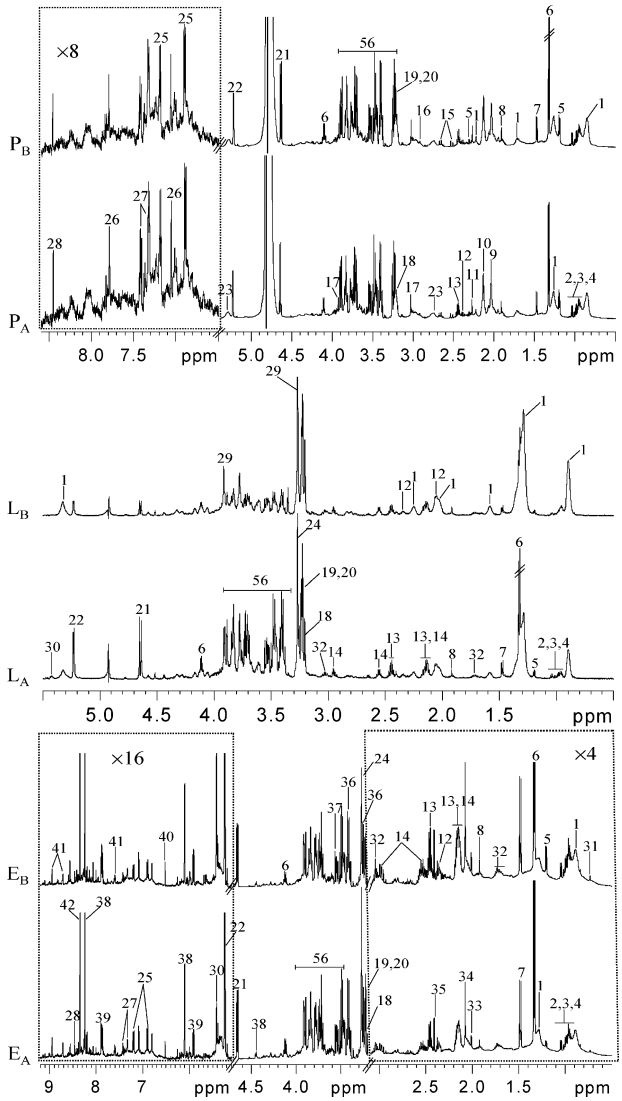


**Figure 2.** Representative 600 MHz $^1$H CPMG NMR spectra of rat blood plasma (P), liver tissue (L), and liver aqueous extracts (E) from the control group (A) and treated with AFB1 (B). The region of $\delta$ 6.0−8.52 in the blood plasma spectra was vertically expanded 8 times compared with the region of $\delta$ 0.5−5.4. The regions of $\delta$ 9.2−5.1 and $\delta$ 3.1−0.5 in the liver aqueous extracts spectra were vertically expanded 16 and 4 times compared with the region of $\delta$ 0.5−4.7. Keys: 1, lipid; 2, isoleucine; 3, leucine; 4, valine; 5, D-3-hydroxybutyrate; 6, lactate; 7, alanine; 8, acetate; 9, *N*-acetyl-glycoproteins; 10, *O*-acetyl-glycoproteins; 11, acetoacetate; 12, glutamate; 13, glutamine; 14, glutathione; 15, citrate; 16, dimethylglycine; 17, creatine; 18, choline; 19, phosphorylcholine; 20, glycerophosphocholine; 21, $\beta$-glucose; 22, $\alpha$-glucose; 23, unsaturated fatty acid; 24, TMAO; 25, tyrosine; 26, histidine; 27, phenylalanine; 28, formate; 29, betaine; 30, glycogen; 31, bile acid; 32, lysine; 33, *N*-acetyl aspartate; 34, residual acetonitrile; 35, succinate; 36, taurine; 37, glycine; 38, inosine; 39, uridine; 40, fumarate; 41, nicotinurate; 42, adenosine; 56, glucose and amino acids $\alpha$-CH resonances.

From the third day after AFB1-treatment, obvious changes were observable for the levels of a number of endogenous metabolites such as hippurate, 2-oxoglutarate, and citrate. To extract the detailed information about AFB1-induced metabolic alterations, multivariate data analysis of these NMR profiles was performed.

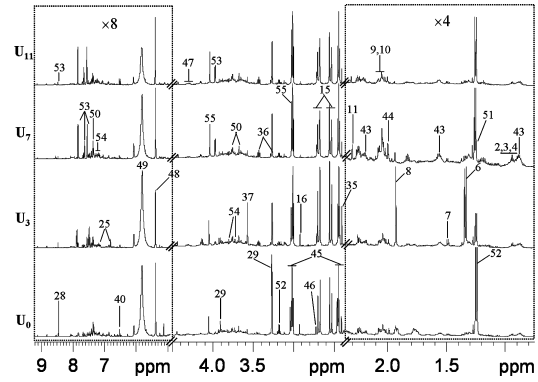


**Figure 3.** Typical 600 MHz $^1$H NMR spectra of urine collected from an AFB1-treated rat at predose ($U_0$), day 3 ($U_3$), day 7 ($U_7$), and day 11 ($U_{11}$). The region of $\delta$ 9.2−5.2 in the urine spectra was vertically expanded 8 times compared with the region of $\delta$ 0.5−4.5. Key: 43, butyrate; 44, acetamide; 45, 2-oxoglutarate; 46, dimethylamine; 47, malate; 48, allantoate; 49, urea; 50, phenylacetylglycine; 51, 3-hydroxy-isovalerate; 52, methylmalonate; 53, hippurate; 54, indoleacetylglycine; 55, creatinine. The other keys are shown in Supporting Information Table S2.

**AFB1-Induced Metabonomic Changes.** PCA of the normalized NMR data from plasma, liver tissue, liver extraction, and urine samples was conducted. One plasma sample from the AFB1-treated group appeared to be an outlier (data not shown) with a high concentration of lactate; therefore, this sample was excluded from subsequent analysis. No outliers were observed for liver tissue, liver extracts, and urine samples. Comparative O-PLS-DA was conducted between the NMR data from the AFB1-dosed and control rats at matched time points for individual biological matrices. The values for $R^2$ and $Q^2$ were employed as initial indicators for the model qualities indicating goodness of fit and predictability of the models (Table 1).

AFB1-treated rats showed significant differences from controls in the $^1$H NMR profiles of plasma, liver tissues, and liver extracts as suggested by the cross-validated model parameters (Table 1) and the results of permutation tests (Supporting Information Figure S1a−c). The dominant metabolites for the differentiation were shown in the O-PLS-DA coefficient plots (Figure 4,$P_2$, $L_2$, and $E_2$). Compared with the control rats, AFB1 treated animals have significant lower levels of lipids, 3-HB, and citrate in plasma, and higher levels of glucose, *O*-acetyl glycoproteins (OAG), acetate, formate, tyrosine, and membrane related metabolites (choline, PC, and GPC).

Metabolic profiles of intact liver tissues were also markedly altered following AFB1 exposure as illustrated in the cross-validated O-PLS-DA coefficient plot (Figure 4, $L_2$). AFB1 exposure significantly elevated the levels of lipid moieties, acetate, choline, PC, GPC, TMAO, betaine, and 3-HB but significantly decreased the levels of hepatic glucose and glycogen. Similar to the metabolic profiles of intact liver tissues, significant changes were observed in the liver extracts (Figure 4, $E_2$). Such changes were highlighted with elevation of choline, PC, GPC, TMAO, betaine, 3-HB, glutathione, a range of amino acids, and the nucleotide metabolites (e.g., inosine and uridine) and nicotinurate; decline of glucose, glycogen, and lactate in the liver extracts from AFB1 treated rats were also observed.

The same O-PLS-DA strategy was further applied to the urinary metabolic profiles of the controls and ABF1-treated rats over 6 matched time points (day 1, 3, 5, 7, 9, and 11 postdose, respectively). All models were rigorously evaluated with per-

**Table 1.** Significantly Changed Metabolites in the Plasma, Intact Liver Tissue and Aqueous Extract of Liver from Rats Exposed to AFB1[a]

| Aflatoxin B1 exposure (0.32 mg/(kg/day); correlation coefficient, $\|r\| > 0.514$, $p < 0.05$) | | | | |
|---|---|---|---|---|
| key | metabolites | blood plasma ($R^2X = 0.39$; $Q^2 = 0.62$) | liver tissue ($R^2X = 0.38$; $Q^2 = 0.56$) | aqueous liver extract ($R^2X = 0.78$; $Q^2 = 0.772$) |
| 1 | Lipid | −0.58 | +0.78 | |
| 2 | Isoleucine | — | — | +0.81 |
| 3 | Leucine | — | — | +0.82 |
| 4 | Valine | — | — | +0.82 |
| 5 | 3-HB | −0.53 | +0.71 | +0.76 |
| 6 | Lactate | +0.35 | — | −0.56 |
| 7 | Alanine | — | — | +0.52 |
| 8 | Acetate | +0.56 | +0.63 | +0.81 |
| 10 | OAG | +0.62 | | |
| 12 | Glutamate | — | | +0.88 |
| 13 | Glutamine | — | | +0.87 |
| 14 | Glutathione | | | +0.87 |
| 15 | Citrate | −0.52 | | |
| 18 | Choline | +0.52 | +0.83 | +0.89 |
| 19 | PC | +0.52 | +0.76 | +0.90 |
| 20 | GPC | +0.53 | +0.75 | +0.88 |
| 21 | $\beta$-Glucose | +0.54 | −0.89 | −0.90 |
| 22 | α-Glucose | +0.54 | −0.81 | |
| 24 | TMAO | | +0.54 | +0.60 |
| 25 | Tyrosine | +0.55 | | +0.75 |
| 26 | Histidine | | | +0.73 |
| 27 | Phenylalanine | | | +0.78 |
| 28 | Formate | +0.52 | | +0.76 |
| 29 | Betaine | | +0.54 | +0.61 |
| 30 | Glycogen | | −0.53 | |
| 32 | Lysine | | | +0.72 |
| 37 | Glycine | | | +0.76 |
| 38 | Inosine | | | +0.81 |
| 39 | Uridine | | | +0.81 |
| 41 | Nicotinurate | | | +0.83 |
| 42 | Adenosine | | | +0.73 |

[a] Numbers correspond to the metabolite peak positions on NMR spectra in Figure 2 or Table S2; the correlation coefficients shown are based on O-PLS-DA analysis of a two-class model (control and AFB1 exposure group), positive and negative value indicate an increase and decrease of metabolite in the AFB1 exposure group relative to control rats. Abbreviations: OAG, *O*-acetyl-glycoproteins; PC, Phosphocholine; GPC, Glycerophosphocholine; TMAO, Trimethylamine-*N*-oxide.

mutation tests with 200 permutations (Supporting Information Figure S1). The correlation coefficient plots (Figure 5) indicated the discriminating variables for the separation between control and AFB1-treated groups. Compared with the controls, AFB1 exposure resulted in significant decreases in the levels of 2-oxoglutarate and citrate from day 3 to day 9 together with an increase in level of hippurate from day 3 to day 7. AFB1 also caused higher urinary excretion of phenylacetylglycine (PAG), indoleacetylglycine (IAG), creatinine, fumarate, and acetoacetate, but lower excretions of butyrate, methylmalonate, and lactate from day 9 to day 11 (Table 2).

Figure 6 shows the AFB1-induced dynamic concentration variations for some urinary metabolites representing different pathways, which was calculated as the concentration ratios from urines of the AFB1-treated rats against those from the controls. Urinary citrate and 2-oxoglutarate from AFB1 treated rats exhibited similar trends, with their depletion at early stage of exposure (day 1−7); such changes reversed at the later stage of exposure (day 9−11). In contrast, AFB1 caused a steady increase in urinary hippurate, PAG, and IAG with a marked increase in the levels of hippurate between day 5−9 of continuous AFB1 exposure and substantial elevation of PAG and IAG between day 9−11 of AFB1 exposure. The recoveries for the AFB1-induced changes in citrate, oxoglutatrate, and hippurate suggest that there may be some adaptive responses from liver although such recovery will be of interests for the future investigations.

## Discussions

The aim of the current study is to investigate metabolic consequences of AFB1 exposure in a holistic manner by employing a metabonomic strategy. We examined metabolic alterations in extensive biological matrices including plasma and liver after 12 days of continuous dosing AFB1 and urine samples at day 1, 3, 5, 7, 9, and 11 during the treatments. The effects of AFB1 on rat liver were investigated for both metabolic profiles of intact liver tissues and aqueous extracts, so that complementary information was obtained. No significant changes were observed for the AFB1 effects on the kidney metabolic features. The above results indicated that AFB1 exposure caused significant liver injury and comprehensive metabolic alterations in urine, plasma, and liver tissues involving many related metabolic pathways (Figure 7).

**Liver Injuries.** The dosage of AFB1 in the current work (0.32 mg/(kg body weight/day)) can be regarded as a moderate (or intermediate) dosage, whereas the literature has reported high (3 mg/kg body weight, i.p.)[35] and low dosages (55 $\mu$g/(kg body weight/day)).[36] Treatment with a moderate dosage of AFB1 induced liver injuries in the morphological level with the formation of hepatic vacuole and lipid droplets (Figure 1). Vacuole formation in the periportal hepatocytes of rat liver exposed to a much higher dosage AFB1 (3 mg/kg) was previously observed with *in vivo* MRI assessment.[35] Such vacuole formation is often followed by hepatocellular necrosis, membrane disruption and nuclear disintegration. These further cause massive water and iron influxes, which subsequently lead to severe stresses to mitochondrial and endoplasmic reticulum.[37,38] Vacuole formation associated with swelling of hepatocytes has also been reported for the effects of other hepatotoxins such as halothane and carbon tetrachloride ($CCl_4$).[39,40]

From a metabolism point of view, the observation of elevated levels of OAG, choline, PC, GPC, TMAO, and betaine is consistent with the swelling of hepatocytes. The OAG in rat blood plasma was associated with inflammation of injured tissue and represented "acute-phase" glycoproteins in model animals under inflammatory conditions.[41] Consistently higher levels of membrane moieties, such as choline, PC, and GPC found in the rat liver and plasma exposed to AFB1 in the current investigation also agree well with the swelling of hepatocytes because choline, PC, and GPC are essential elements for structural integrity of cell membranes.[42] The swelling of hepatocytes also leads to the accumulation of intracytoplasmic fluids in cells, and in order to maintain osmolarity and protect cell damage in hypotonic conditions, several organic osmolytes, such as TMAO and betaine, were elevated in liver.[43] Liver injuries induced by AFB1 exposure was further confirmed by significant increases in ALT and AST (Table S1).

Supportive evidence of liver damage by AFB1 exposure could also be found in gene expression of liver obtained from rats dosed with AFB1 for 14 days (0.24 mg/(kg/day)), where genes encoding cytoskeleton formation were up-regulated, including CRYAB α B-Crystallin, RhoB, SPTA2 spectrin α chain (fodrin α chain), and TMSB 10 thymosin $\beta$-10.[44] In addition, gene

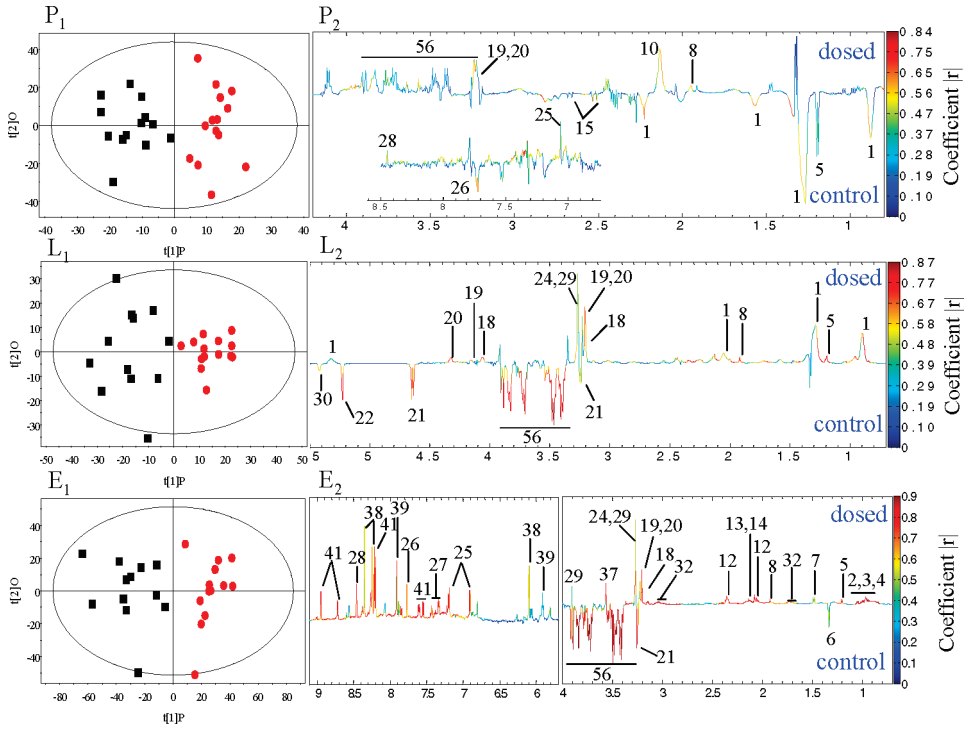


**Figure 4.** O-PLS-DA scores ($P_1$, $L_1$, $E_1$) and coefficient-coded loadings plots ($P_2$, $L_2$, $E_2$) for the models discriminating the control (black squares) and AFB1 treated groups (red dots) from data for plasma ($P_1$, $P_2$), liver tissue ($L_1$, $L_2$), and liver aqueous extracts ($E_1$, $E_2$). Metabolite keys to the number are shown in Figure 2 and Table S2.

expression of an inflammatory response level, TAP1 antigen peptide transporter 1, was up-regulated in the rats exposed to AFB1.[44]

In urine, we noted elevated levels of hippurate, phenylacetylglycine (PAG), and indoleacetylglycine (IAG) in the dosed rats at different time points, suggesting that AFB1 exposure promoted glycine conjugation (Figure 7). This is because the liver has a major role in conjugation of benzoic acid, phenylacetic acid, and indoleacetic acid with glycine to produce hippurate, PAG, and IAG.[45] Previous reports suggested that elevated levels of urinary PAG exhibited in abnormal phospholipid accumulated rat liver and may be useful as a surrogate biomarker for associated changes in gut microbeota.[47,55] Acyl-CoA has a major role in glycine conjugation;[46] however, no report has shown that this enzyme was modified by AFB1 exposure. Therefore, the newly found AFB1-induced alterations of urinary hippurate, PAG, and IAG were not only reflective of liver dysfunction, but variations of these urinary aromatic metabolites were frequently related to modulation of activity or population of gut microbiota.[48,49] Therefore, AFB1 exposure may have also caused changes in gut microbiota, which warrants further investigation to address the challenges to microbiome.

**Lipid Metabolism and Oxidation.** One of the most prominent findings in the current investigation was hepatic lipidosis, which was accompanied by decreased levels of lipids in plasma (Figure 7). This observation appeared to be a common cellular response to a number of liver toxic compounds, such as allyl formate,[21] acetaminophen,[27] and ethionine.[50] The hepatic lipidosis caused by AFB1 exposure (Figure 1, 4, Table 1) may also be due to the reduced alterations in lipid transportation from liver to the plasma as in the case of the hepatic lipidosis induced by allyl formate,[21] perfluorododecanoic acid (PFDoA),[28] and ethionine.[50] This is consistent with the down-regulation of genes related to transportation of lipid out of the hepatic cells in male broiler chicks fed with AFB1.[51]

Furthermore, we observed increased levels of ketone bodies, such as 3-HB in the liver and acetoacetate in urine, from the dosed rats. These ketone bodies are the products of $\beta$-oxidation of fatty acid in mitochondria and elevations of them suggested the promoted $\beta$-oxidation of fatty acid with AFB1 exposure (Figure 7). In agreement with our findings, previous investigation found that AFB1 exposure caused up-regulation of peroxisome proliferator-activated receptor α (PPARα), a key regulator for lipid metabolism.[51] In addition, we also noted an elevated concentration of acetate, which is the end product of fatty acid oxidation in peroxisomes.[52]

Lipid oxidation often leads to generation of hydrogen peroxides, a cause for free radical oxidative damage. Oxidative stress followed by lipid oxidation has previously been reported in AFB1 toxicity; reactive oxygen species (ROS), such as $H_2O_2$ and $O_2^-$, are widely considered to participate in the main mechanism of aflatoxin toxicity.[9] Oxidative stress ultimately triggers an antioxidative response of an organism. Here we observed elevated levels of glutathione in the rat liver exposed to AFB1, which is consistent with antioxidative responses activated by AFB1. Previous supportive evidence comes from AFB1-induced up-regulation of gene expressions for $\gamma$-glutamyltranspeptidase and glutathione-*S*-transferase in rats.[44,53] The notion of AFB1-induced oxidative stresses was further supported by the observation of the AFB1-induced up-regulation of other genes related to antioxidant response, such as NADPH quinone oxidoreductase (diaphorase)[44] and heme oxygenase,[51] in rats and male chicks.

**Glucose and Glycogen Metabolism.** Compared with controls, rats administered with AFB1 exhibited significantly reduced hepatic glucose/glycogen levels and an elevation of plasma glucose (Figure 7). Such depletion of hepatic glucose has also been observed in human HCC[25] and rats dosed with PFDoA.[28] Our observation suggested that one of the consequences of AFB1 exposure is accelerated rates of glycogenolysis

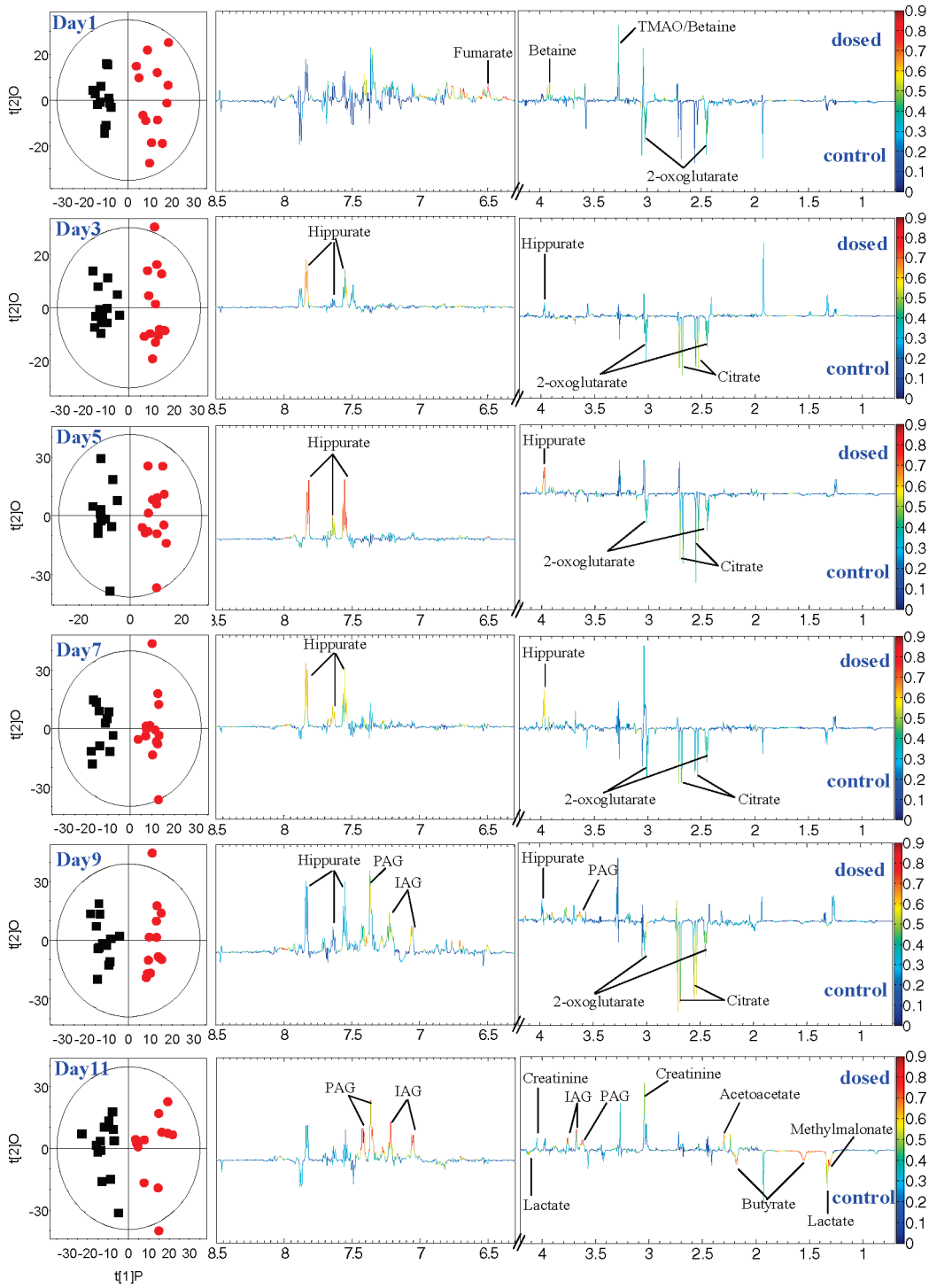


**Figure 5.** O-PLS-DA cross validated scores and loading plots derived from $^{1}$H NMR spectra of urine collected from control rats (black squares) and AFB1 treatment rats (red dots) at various time points.

and glycolysis. There was a trend of increase in lactate concentrations in the plasma of dosed rats, which further supported this notion. In consistence with this finding, the increase of glucose utilization was found to be a major metabolic effect at acute mycotoxin exposure levels.[17] Previous investigation also reported that several enzymes metabolizing glycogen, such as glucose 6-phosphate dehydrogenase, were up-regulated following AFB1 exposure.[54] Moreover, genes involved in carbohydrate metabolism were also up-regulated after AFB1 exposure, for example, glycogen synthase l, GTP cyclohydrolase 1 feedback regulator, and lactate dehydrogenase H subunit.[51]

The depletion of urinary citrate and 2-oxoglutarate in the AFB1 treated rats (Figure 6) suggests an alteration of TCA cycle (Figure 7). Previous studies indicated AFB1-induced hepatotoxicity was initiated by an inhibition of mitochondrial respiratory function, which inevitably led to the changes in the TCA cycle intermediates in the urinary profile.[14,17] Similar observations have been reported in the cases of hepatotoxicity induced by acetaminophen[27] and allyl formate.[21]

**Table 2.** Significant Changes in Urinary Metabolites of Rats Exposed to AFB1 Compared to Controls on Different Days of Treatment[a]

| | Aflatoxin B1 exposure (0.32 mg/(kg/day); $\|r\| > 0.514$, $p < 0.05$) | | | | | |
|---|---|---|---|---|---|---|
| metabolites | Day 1 $R^2X = 0.45$ $Q^2 = 0.59$ | Day 3 $R^2X = 0.56$ $Q^2 = 0.63$ | Day 5 $R^2X = 0.63$ $Q^2 = 0.78$ | Day 7 $R^2X = 0.65$ $Q^2 = 0.54$ | Day 9 $R^2X = 0.55$ $Q^2 = 0.69$ | Day 11 $R^2X = 0.47$ $Q^2 = 0.62$ |
| 2-oxoglutarate | −0.54 | −0.55 | −0.58 | −0.58 | −0.63 | — |
| Citrate | — | −0.64 | −0.62 | −0.65 | −0.68 | — |
| Fumarate | +0.72 | — | — | — | — | — |
| Hippurate | — | +0.63 | +0.66 | +0.74 | +0.61 | — |
| PAG | — | — | — | — | +0.73 | +0.76 |
| IAG | — | — | — | — | +0.74 | +0.78 |
| Creatinine | — | — | — | — | — | +0.57 |
| Betaine | +0.52 | — | — | — | — | — |
| Lactate | — | — | — | — | — | −0.62 |
| Methylmalonate | — | — | — | — | — | −0.79 |
| Butyrate | — | — | — | — | — | −0.75 |
| Acetoacetate | — | — | — | — | — | +0.64 |

[a] Abbreviations: PAG, Phenylacetylglycine; IAG, Indoleacetylglycine.

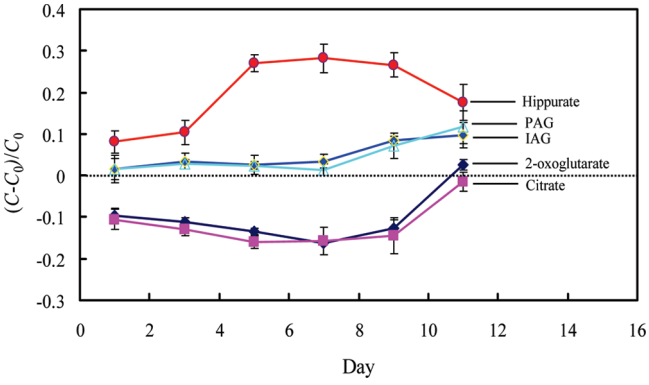


**Figure 6.** Time course of variations for citrate, 2-oxoglutarate, hippurate, PAG, and IAG. The values shown on the vertical-axis are the ratios of metabolite variation induced by AFB1 exposure relative to control group. The error bars represent standard deviations (from 13 biological samples).

**Amino Acid and Nucleotide Metabolism.** AFB1 induced a significant increase in the levels of a range of amino acids in the liver, including tyrosine, phenylalanine, alanine, glutamine, glycine, leucine/isoleucine, and valine. This implies that AFB1 causes disruptions to hepatic amino acid metabolisms. This is consistent with the AFB1-induced up-regulation of gene expression for glutamine synthetase and down-regulations of gene expression for ornithine aminotransferase, betaine-homocysteine *S*-methyltransferase, and glycine-*N*-methyltransferase in male chicks[51] and rats.[44]

Another prominent finding of the present study is the marked elevation in levels of free nucleosides, such as inosine, adenosine, and uridine, in the aqueous liver extracts from rats exposed to AFB1 (Figure 7). This implies AFB1 exposure may cause the degradation of nucleic acids or inhibit the synthesis of DNA and RNA as these metabolites are the basic structural units for nucleic acids. Previous findings in rats supported such

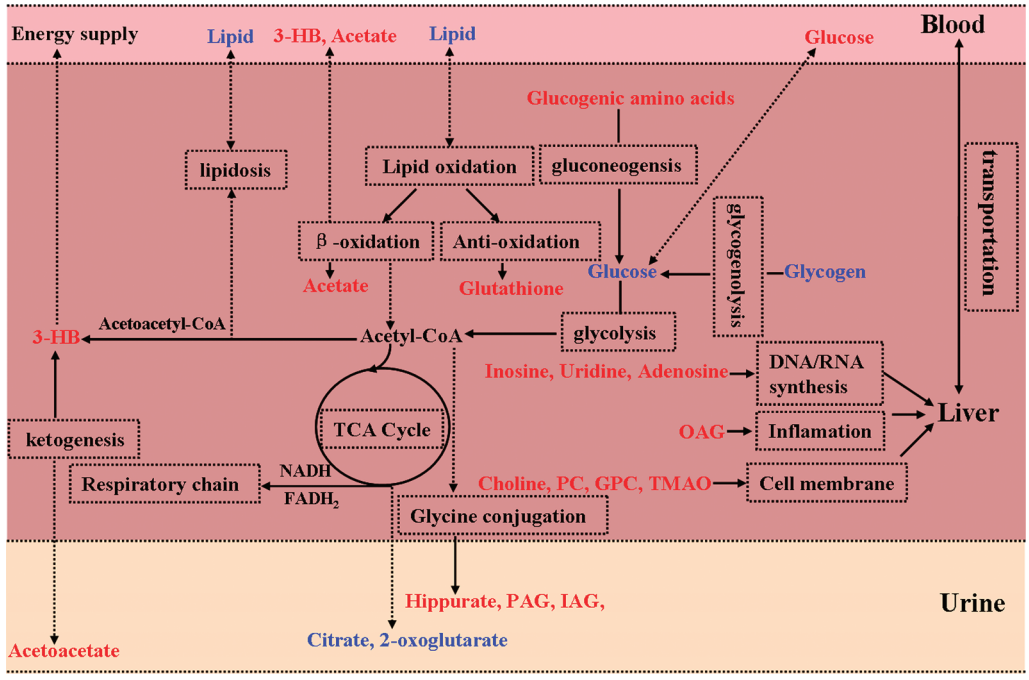


**Figure 7.** The summarized variations of metabolic pathways and related metabolites in rats exposed to AFB1. Metabolites in red or blue represent a higher or lower level in respective biological matrices (plasma, liver, and urine) obtained from AFB1-treated rats compared with control rats.

notions with AFB1-induced up-regulation of genes encoding DNA damage responses including O6-methylguanine-DNA methyltransferase, Cyclin G1, B-cell translocation gene 2, cell growth regulatory gene 1, cyclin-dependent kinase inhibitor 1A (p21), thymidylate synthase, and Bc12-associated x protein.[44] Further supportive evidence comes from a previous report that AFB1 metabolite, AFB1-*exo*-8,9-epoxide, bound with guanine residues of DNA,[7] leading to the impairment of DNA and RNA template activity and inhibition of DNA and RNA synthesis.[14]

## Conclusion

Exposure with moderate AFB1 dosage induced obvious liver damages and significant alterations in several metabolic pathways, including increased lipid oxidation, perturbed TCA cycle, disrupted carbohydrate, and amino acid metabolisms as well as inhibition of nucleic acid synthesis (Figure 7). Such toxicity may also cause disruptions of gut microbiota functions. Our results have shown that an integrated NMR analysis of multiple biological matrices, such as plasma, liver, and urine samples, together with histological assessments and traditional clinical biochemical assays provided a holistic method for elucidating mechanisms of a toxic insult. Further investigation on the relationship between AFB1 intakes and the gut microbiota responses will enrich our understandings of the mechanistic aspects of AFB1 toxicity.

**Acknowledgment.** We acknowledge financial supports from National Basic Research Program of China (2009CB118804, 2007CB914701), the National Natural Science Foundation of China (20825520, 20921004) and Chinese Academy of Sciences (KJCX2-YW-W11, KSCX2-YW-N-033). We also thank Dr. Hang Zhu of Wuhan Institute of Physics and Mathematics for developing MATLAB scripts used for color-coded O-PLS-DA coefficient plots, which is based on a script originally downloaded from http://www.mathworks.com/matlabcentral/fileexchange.

**Supporting Information Available:** Table S1, clinical serum biochemistry parameters of rats exposed to AFB1. Table S2, $^1$H NMR data and assignments of the metabolites in rat plasma, urine, liver tissue and liver aqueous extracts. Figure S1, permutation test plots for all the biological matrices. This material is available free of charge via the Internet at http://pubs.acs.org.

## References

(1) Holmquist, G. U.; Walker, H. W.; Stahr, H. M. Influence of temperature, pH, water activity and antifungal agents on growth of aspergillus flavus and A. parasiticus. *J. Food Sci.* **1983**, *48*, 778–782.
(2) Bullerman, L. B. Mycotoxins and food safety. *Food Technol.* **1986**, *40*, 59–66.
(3) Wild, C. P.; Hall, A. J. Primary prevention of hepatocellular carcinoma in developing countries. *Mutat. Res., Rev. Mutat. Res.* **2000**, *462*, 381–393.
(4) Diaz, D. E. A Review on the use of mycotoxin sequestering agents in agricultural livestock production. In *Food Contaminants: Mycotoxins and Food Allergens*; Siantar, D. et al., Eds; ACS Symposium Series Vol *1001*; American Chemical Society: Washington DC, 2008; pp 125−150.
(5) Abdel-Wahhab, M. A.; Nada, S. A.; Farag, I. M.; Abbas, N. F.; Amra, H. A. Potential protective effect of HSCAS and bentonite against dietary aflatoxicosis in rat: with special reference to chromosomal aberrations. *Nat. Toxins* **1998**, *6*, 211–218.
(6) Wogan, G. N.; Newberne, P. M.; Edwards, G. S. Structure-activity relationships in toxicity and carcinogenicity of aflatoxins and analogs. *Cancer Res.* **1971**, *31*, 1936–1942.
(7) Iyer, R. S.; Coles, B. F.; Raney, K. D.; Thier, R.; Guengerich, F. P.; Harris, T. M. DNA adduction by the potent carcinogen aflatoxin B1: mechanistic studies. *J. Am. Chem. Soc.* **1994**, *116*, 1603–1609.
(8) Renzulli, C.; Galvano, F.; Pierdomenico, L.; Speroni, E.; Guerra, M. C. Effects of rosmarinic acid against aflatoxin B1 and ochratoxin A-induced cell damage in a human hepatoma cell line (Hep G2). *J. Appl. Toxicol.* **2004**, *24*, 289–296.
(9) Gesing, A.; Karbownik-Lewinska, M. Protective effects of melatonin and N-acetylserotonin on aflatoxin B1-induced lipid peroxidation in rats. *Cell Biochem. Funct.* **2008**, *26*, 314–319.
(10) Gallagher, E. P.; Wienkers, L. C.; Stapleton, P. L.; Kunze, K. L.; Eaton, D. L. Role of human microsomal and human complementary DNA-expressed cytochromes P4501A2 and P4503A4 in the bioactivation of aflatoxin B1. *Cancer Res.* **1994**, *54*, 101–108.
(11) Kamdem, L. K.; Meineke, I.; Godtel-Armbrust, U.; Brockmoller, J.; Wojnowski, L. Dominant contribution of P450 3A4 to the hepatic carcinogenic activation of aflatoxin B1. *Chem. Res. Toxicol.* **2006**, *19*, 577–586.
(12) Hayes, J. D.; Judah, D. J.; Neal, G. E. Resistance to aflatoxin B1 is associated with the expression of a novel aldo-keto reductase which has catalytic activity towards a cytotoxic aldehyde-containing metabolite of the Toxin. *Cancer Res.* **1993**, *53*, 3887–3894.
(13) Scholl, P. F.; McCoy, L.; Kensler, T. W.; Groopman, J. D. Quantitative analysis and chronic dosimetry of the aflatoxin B1 plasma albumin adduct lys-AFB1 in rats by isotope dilution mass spectrometry. *Chem. Res. Toxicol.* **2005**, *19*, 44–49.
(14) Mclean, M.; Dutton, M. F. Cellular Interactions and metabolism of aflatoxin: an update. *Pharmacol. Ther.* **1995**, *65*, 163–192.
(15) Bedard, L. L.; Massey, T. E. Aflatoxin B1-induced DNA damage and its repair. *Cancer Lett.* **2006**, *241*, 174–183.
(16) Zhang, Y. J.; Chen, C. J.; Haghighi, B.; Yang, G. Y.; Hsieh, L. L.; Wang, L. W.; Santella, R. M. Quantitation of aflatoxin B1-DNA adducts in woodchuck hepatocytes and rat liver tissue by indirect immunofluorescence analysis. *Cancer Res.* **1991**, *51*, 1720–1725.
(17) Kiessling, K. H. Biochemical mechanism of action of mycotoxins. *Pure Appl. Chem.* **1986**, *58*, 327–338.
(18) Hsieh, L. L.; Hsu, S. W.; Chen, D. S.; Santella, R. M. Immunological detection of aflatoxin B1-DNA adducts formed *in vivo*. *Cancer Res.* **1988**, *48*, 6328–6331.
(19) Carvajal, M. Aflatoxin-DNA adducts as biomarkers of cancer: nature, formation, kinds of AF-DNA adducts, methodology, effects and control. In *Food Contaminants: Mycotoxins and Food Allergens*; Siantar, D. et al, Eds; ACS symposium Series Vol *1001*; American Chemical Society: Washington, DC, 2008; pp 13−55.
(20) Ebbels, T. M.; Keun, H. C.; Beckonert, O. P.; Bollard, M. E.; Lindon, J. C.; Holmes, E.; Nicholson, J. K. Prediction and classification of drug toxicity using probabilistic modeling of temporal metabolic data: the consortium on metabonomic toxicology screening approach. *J. Proteome Res.* **2007**, *6*, 4407–4422.
(21) Yap, I. K.; Clayton, T. A.; Tang, H.; Everett, J. R.; Hanton, G.; Provost, J. P.; Le Net, J. L.; Charuel, C.; Lindon, J. C.; Nicholson, J. K. An integrated metabonomic approach to describe temporal metabolic disregulation induced in the rat by the model hepatotoxin allyl formate. *J. Proteome Res.* **2006**, *5*, 2675–2684.
(22) Wojnowski, L.; Turner, P. C.; Pedersen, B.; Hustert, E.; Brockmoller, J.; Mendy, M.; Whittle, H. C.; Kirk, G.; Wild, C. P. Increased levels of aflatoxin-albumin adducts are associated with CYP3A5 polymorphisms in The Gambia, West Africa. *Pharmacogenetics* **2004**, *14*, 691–700.
(23) Waters, N. J.; Holmes, E.; Williams, A.; Waterfield, C. J.; Farrant, R. D.; Nicholson, J. K. NMR and pattern recognition studies on the time-related metabolic effects of α-Naphthylisothiocyanate on liver, urine, and plasma in the rat: an integrative metabonomic approach. *Chem. Res. Toxicol.* **2001**, *14*, 1401–1412.
(24) Azmi, J.; Griffin, J. L.; Shore, R. F.; Holmes, E.; Nicholson, J. K. Chemometric analysis of biofluids following toxicant induced hepatotoxicity: A metabonomic approach to distinguish the effects of 1-naphthylisothiocyanate from its products. *Xenobiotica* **2005**, *35*, 839–852.
(25) Yang, Y.; Li, C.; Nie, X.; Feng, X.; Chen, W.; Yue, Y.; Tang, H.; Deng, F. Metabonomic studies of human hepatocellular carcinoma using high-resolution magic-angle spinning $^1$H NMR spectroscopy in conjunction with multivariate data analysis. *J. Proteome Res.* **2007**, *6*, 2605–2614.
(26) Garrod, S.; Bollard, M. E.; Nicholls, A. W.; Connor, S. C.; Connelly, J.; Nicholson, J. K.; Holmes, E. Integrated metabonomic analysis of the multiorgan effects of hydrazine toxicity in the rat. *Chem. Res. Toxicol.* **2005**, *18*, 115–122.
(27) Coen, M.; Lenz, E. M.; Nicholson, J. K.; Wilson, I. D.; Pognan, F.; Lindon, J. C. An integrated metabonomic investigation of acetami-

nophen toxicity in the mouse using NMR spectroscopy. *Chem. Res. Toxicol.* **2003**, *16*, 295–303.
(28) Ding, L.; Hao, F.; Shi, Z.; Wang, Y.; Zhang, H.; Tang, H.; Dai, J. Systems biological responses to chronic perfluorododecanoic acid exposure by integrated metabonomic and transcriptomic studies. *J. Proteome Res.* **2009**, *8*, 2882–2891.
(29) Xiao, C.; Hao, F.; Qin, X.; Wang, Y.; Tang, H. An optimized buffer system for NMR-based urinary metabonomics with effective pH control, chemical shift consistency and dilution minimization. *Analyst* **2009**, *134*, 916–925.
(30) Dai, H.; Xiao, C.; Liu, H.; Tang, H. Combined NMR and LC-MS analysis reveals the metabonomic changes in Salvia miltiorrhiza Bunge induced by water depletion. *J. Proteome Res.* **2010**, *9*, 1460–1475.
(31) Dai, H.; Xiao, C.; Liu, H.; Hao, F.; Tang, H. Combined NMR and LC-DAD-MS analysis reveals comprehensive metabonomic variations for three phenotypic cultivars of Salvia Miltiorrhiza Bunge. *J. Proteome Res.* **2010**, *9*, 1565–1578.
(32) Trygg, J.; Wold, S. Orthogonal projections to latent structures (O-PLS). *J. Chemom.* **2002**, *16*, 119–128.
(33) Eriksson, L.; Andersson, P. L.; Johansson, E.; Tysklind, M. Megavariate analysis of environmental QSAR data. Part I: A basic framework founded on principal component analysis (PCA), partial least squares (PLS), and statistical molecular design (SMD). *Mol. Diversity* **2006**, *10*, 169–186.
(34) Tang, H.; Wang, Y.; Nicholson, J. K.; Lindon, J. C. Use of relaxation-edited one-dimensional and two dimensional nuclear magnetic resonance spectroscopy to improve detection of small metabolites in blood plasma. *Anal. Biochem.* **2004**, *325*, 260–272.
(35) Towner, R. A.; Hashimoto, H.; Summers, P. M. Non-invasive *in vivo* magnetic resonance imaging assessment of acute aflatoxin B1 hepatotoxicity in rats. *Biochim. Biophys. Acta, Gen. Subj.* **2000**, *1475*, 314–320.
(36) Guengerich, F. P.; Arneson, K. O.; Williams, K. M.; Deng, Z.; Harris, T. M. Reaction of aflatoxin B1 oxidation products with lysine. *Chem. Res. Toxicol.* **2002**, *15*, 780–792.
(37) Choo, K. B.; Chen, C. M.; Han, C. P.; Cheng, W. T. K.; Au, L. C. Molecular analysis of cellular loci disrupted by papillomavirus 16 integration in cervical cancer: Frequent viral integration in topologically destabilized and transcriptionally active chromosomal regions. *J. Med. Virol.* **1996**, *49*, 15–22.
(38) Bisgaard, H. C. Thorgeirsson, S. S.Hepatic regeneration: the role of regeneration in pathogenesis of chronic liver diseases. *Clin. Lab. Med.* **1996**, *16*, 325–339.
(39) Mion, F.; Geloen, A.; Rousseau, M.; Brazier, J. L.; Minaire, Y. Mechanism of carbon-tetrachloride autoprotection: an *in vivo* study based on $^{13}$C-aminopyrine and $^{13}$C-galactose breath tests. *Life Sci.* **1994**, *54*, 2093–2098.
(40) Manno, M.; Ferrara, R.; Cazzaro, S.; Rigotti, P.; Ancona, E. Suicidal inactivation of human cytochrome-P450 by carbon-tetrachloride and halothane *in vitro*. *Pharmacol. Toxicol.* **1992**, *70*, 13–18.
(41) Grootveld, M.; Claxson, A. W.; Chander, C. L.; Haycock, P.; Blake, D. R.; Hawkes, G. E. High resolution proton NMR investigations of rat blood plasma: assignment of resonances for the molecularly mobile carbohydrate side-chains of acute-phase glycoproteins. *FEBS Lett.* **1993**, *322*, 266–276.
(42) Klein, J. Membrane breakdown in acute and chronic neurodegeneration: focus on choline-containing phospholipids. *J. Neural Transm.* **2000**, *107*, 1027–1063.
(43) Zerbst-Boroffka, I.; Kamaltynow, R. M.; Harjes, S.; Kinne-Saffran, E.; Gross, J. TMAO and other organic osmolytes in the muscles of amphipods (Crustacea) from shallow and deep water of Lake Baikal. *Comp. Biochem. Physiol., Part A: Mol Integr. Physiol.* **2005**, *142*, 58–64.
(44) Ellinger-Ziegelbauer, H.; Stuart, B.; Wahle, B.; Bomann, W.; Ahr, H. J. Characteristic expression profiles induced by genotoxic carcinogens in rat liver. *Toxicol. Sci.* **2004**, *77*, 19–34.
(45) Kasuya, F.; Yamaoka, Y.; Osawa, E.; Igarashi, K.; Fukui, M. Difference of the liver and kidney in glycine conjugation of ortho-substituted benzoic acids. *Chem. Biol. Interact.* **2000**, *125*, 39–50.
(46) Kasuya, F.; Igarashi, K.; Fukui, M. Participation of a medium chain acyl-CoA synthetase in glycine conjugation of the benzoic acid derivatives with the electron-donating groups. *Biochem. Pharmacol.* **1996**, *51*, 805–809.
(47) Monteith, D. K.; Morgan, R. E.; Halstead, B. *In vitro* assays and biomarkers for drug-induced phospholipidosis. *Expert Opin. Drug Metab. Toxicol.* **2006**, *2*, 687–696.
(48) Nicholls, A. W.; Mortishire-Smith, R. J.; Nicholson, J. K. NMR spectroscopic-based metabonomic studies of urinary metabolite variation in acclimatizing germ-free rats. *Chem. Res. Toxicol.* **2003**, *16*, 1395–1404.
(49) Williams, R. E.; Eyton-Jones, H. W.; Farnworth, M. J.; Gallagher, R.; Provan, W. M. Effect of intestinal microflora on the urinary metabolic profile of rats: a $^{1}$H-nuclear magnetic resonance spectroscopy study. *Xenobiotica* **2002**, *32*, 783–794.
(50) Skordi, E.; Yap, I. K.; Claus, S. P.; Martin, F. P.; Cloarec, O.; Lindberg, J.; Schuppe-Koistinen, I.; Holmes, E.; Nicholson, J. K. Analysis of time-related metabolic fluctuations induced by ethionine in the rat. *J. Proteome Res.* **2007**, *6*, 4572–4581.
(51) Yarru, L. P.; Settivari, R. S.; Antoniou, E.; Ledoux, D. R.; Rottinghaus, G. E. Toxicological and gene expression analysis of the impact of aflatoxin B1 on hepatic function of male broiler chicks. *Poult. Sci.* **2009**, *88*, 360–371.
(52) Leighton, F.; Bergseth, S.; Rortveit, T.; Christiansen, E. N.; Bremer, J. Free acetate production by rat hepatocytes during peroxisomal fatty acid and dicarboxylic acid oxidation. *J. Biol. Chem.* **1989**, *264*, 10347–10350.
(53) Manson, M. M.; Hudson, E. A.; Ball, H. W.; Barrett, M. C.; Clark, H. L.; Judah, D. J.; Verschoyle, R. D.; Neal, G. E. Chemoprevention of aflatoxin B1-induced carcinogenesis by indole-3-carbinol in rat liver-predicting the outcome using early biomarkers. *Carcinogenesis* **1998**, *19*, 1829–1836.
(54) Ankrah, N. A.; Wei, R. Effect of a single subtoxic dose of aflatoxin B1 (AFB1) on glucose-6-phosphate dehydrogenase in mouse liver. *Biochem. Pharmacol.* **1987**, *36*, 1181–1182.
(55) Phipps, A. N.; Stewart, J.; Wright, B.; Wilson, I. D. Effect of Diet on the Urinary Excretion of Hippuric Acid and other Dietary-derived Aromatics in the Rat. A Complex Interaction between Diet, Gut Microflora and Substrate Specificity. *Xenobiotica* **1998**, *28*, 527–537.

PR100792Q